Cite this: *Nanoscale*, 2012, **4**, 278

www.rsc.org/nanoscale

PAPER

Fabrication of multi-level carbon nanotube arrays with adjustable patterns†

Jianliang Gong,[a] Lichao Sun,[b] Yawen Zhong,[a] Chunyin Ma,[b] Lei Li,*[a] Suyuan Xie[b] and Vladimir Svrcek[c]

Received 27th August 2011, Accepted 17th October 2011
DOI: 10.1039/c1nr11191d

Multi-level carbon nanotube (CNT) arrays with adjustable patterns were prepared by a combination of the breath figure (BF) process and chemical vapor deposition. Polystyrene-*b*-poly(acrylic acid)/ferrocene was dissolved in carbon disulfide and cast onto a Si substrate covered with a transmission electron microscope grid in saturated relative humidity. A two-level microporous hybrid film with a block copolymer skeleton formed on the substrate after evaporation of the organic solvent and water. One level of ordered surface features originates from the contour of the hard templates; while the other level originates from the condensation of water droplets (BF arrays). Ultraviolet irradiation effectively cross-linked the polymer matrix and endowed the hybrid film with improved thermal stability. In the subsequent pyrolysis, the incorporated ferrocene in the hybrid film was oxidized and turned the polymer skeleton into the ferrous inorganic micropatterns. Either the cross-linked hybrid film or the ferrous inorganic micropatterns could act as a template to grow the multi-level CNT patterns, *e.g.* isolated and honeycomb-structured CNT bundle arrays perpendicular to the substrate.

Introduction

Carbon nanotubes (CNTs) are considered central nanomaterials in the fields of nanoscience and nanotechnology, due to their remarkable electrical, thermal, optical and mechanical properties.[1] In order to integrate CNTs with conventional microelectronics, and to develop novel devices such as emitters and sensors, selective positioning and controlled growth of CNTs are key technologies. Therefore, the fabrication of CNTs with well-defined arrangements and configurations has attracted much attention in the past decade,[2] and specifically, vertical alignment of CNTs has become an important goal due to its technological importance for practical applications including hydrophobic surfaces fabrication, optical devices, nanoscale sensors and electronic circuits, *etc*.[3] Many efforts have been made to synthesize CNTs by chemical vapor deposition (CVD) on large-scaled predesigned catalyst patterns or substrate patterns, which are usually fabricated by offset printing, standard lithography, and soft lithography.[4] By means of these available techniques, the space resolution for the preparation of CNT patterns on the substrate has been down to the micrometre scale. However, the time consuming preparation and high cost of the mentioned technologies are the major disadvantages limiting their practical applications.

In contrast, self-assembly provides efficient and fundamentally simple methods for creating microstructures. The breath figure (BF) process is one of the most promising self-assembling strategies towards large-scaled patterns with an ordered two-dimensional array of holes.[5] In a typical BF process, a water-immiscible solution containing polymer is cast onto the substrate under high humidity. Hexagonally packed water microdroplets form on the solution surface due to the evaporative cooling of the solvent, and are then transferred to the solution front driven by convection flow and the capillary force. After the evaporation of the solvent, the honeycomb-patterned polymer film forms, with the water droplet array filling it as a template. Finally, a microporous polymer film is obtained after water evaporation. Various types of polymers can be fabricated into a honeycomb-patterned film with controlled pore size, ranging from hundreds of nanometres to hundreds of micrometres.[6] This simple method offers new prospects in the field of microporous films, and also opens new routes to the preparation of patterned nano/micro materials in low cost and large scale. Quite recently, we developed a robust static BF process to fabricate honeycomb-structured polymeric films using amphiphilic diblock copolymer polystyrene-*b*-poly(acrylic acid) (PSPAA), hybrid diblock copolymer polydimethylsiloxane-*b*-polystyrene, commercially available triblock copolymers of polystyrene-*b*-polybutadiene-*b*-polystyrene and polystyrene-*b*-polyisoprene-*b*-polystyrene, and linear PS without polar end groups.[7] Particularly, highly ordered microporous hybrid films of polymer/inorganic precursors were also formed in a wide solution concentration range tolerating temperatures, molecular weights and chemical compositions. In the following

[a]*College of Materials, Xiamen University, Xiamen, 361005, P. R. China. E-mail: lilei@xmu.edu.cn; Fax: +86-592-2183937; Tel: +86-592-2186296*
[b]*College of Chemistry and Chemical Engineering, Xiamen University, Xiamen, 361005, P. R. China*
[c]*Next Generation Device Team, Research Center for Photovoltaic Technologies, National Institute of Advanced Industrial Science and Technology (AIST), Central 2, Umezono 1-1-1, Tsukuba, 305-8568, Japan*
† Electronic supplementary information (ESI) available. See DOI: 10.1039/c1nr11191d

ultraviolet irradiation, the polymer matrix was cross-linked and worked as a structure-directing agent during the subsequent pyrolysis process to construct inorganic micropatterns on the substrate. By simply changing the precursor, various functionalized inorganic micropatterns could be created, and were further used to initiate the growth of ZnO nanorods and CNT arrays.[7b,7c]

In this article, based on our previous work, we develop a new method to prepare two-level CNT patterns, using a transmission electron microscope (TEM) grid and honeycomb-patterned polymer film prepared through the BF process. One order level of the CNT pattern originates from the contour of the TEM grid; while the other level originates from the BF arrays. The beauty of this process is that a number of different CNT patterns can be easily obtained by choosing different hard templates. Circumventing expensive lithographic techniques, the reported methodology provides a convenient way to prepare patterned CNTs in large area that may be valuable for the nanoscale engineering applications.

Results and discussion

The fabrication process of multi-level CNT patterns on a Si wafer with the guidance of a template is shown in Fig. 1. Here, TEM grids are employed as templates because they are commercially available and low-cost with variable mesh size and shape. Firstly, a TEM grid was placed on an Si wafer, and a blend solution of PSPAA/ferrocene (5 : 1, w/w) in carbon disulfide (CS_2) was then cast onto this grid by a microsyringe (Fig. 1a). After evaporation of the solvent CS_2 under saturated relative humidity, the substrate was taken out from the water vapor and the TEM grid was carefully peeled off. A highly regular microstructured hybrid film formed on the substrate (Fig. 1b and 1c). The thermal stability of the polymer matrix was further improved through cross-linking induced by ultraviolet irradiation, whereas the honeycomb structures were clearly intact (Fig. 1d). Such a cross-linked hybrid film could then act as the template for CVD growth of isolated CNT bundle arrays in the cavities (Fig. 1e), or serve as the structure-directing model for further preparation of ferrous inorganic micropatterns through pyrolysis (Fig. 1f). In this case the ferrocene was oxidized and replaced the skeleton of the polymer matrix. Guided by these inorganic micropatterns in the mesh spaces, two-level honeycomb-structured dense CNT arrays perpendicular to the substrate could be obtained by CVD growth (Fig. 1g).

The formation of regular BF arrays on nonplanar substrates (guided by placing TEM grids, clay particles or other hard templates on flat surfaces) has been investigated by Qiao *et al.*, by using a library of core cross-linked star polymers with different arm compositions. The glass transition temperature (T_g) of the series of star polymers ranged from −123 to 100 °C. It was found that all the polymers successfully formed ordered microporous films on flat surfaces.[8] However, only the polymers with a T_g below 48 °C could show enough "fluid-like" character to contour the surface features of the nonplanar substrates. For PSPAA, the T_g of PS and PAA are 100 and 102 °C, respectively,[9] thus the PSPAA is not believed to be a good material to form microporous film on the nonplanar surface during the BF process. Astonishingly, scanning electronic microscopy (SEM) images demonstrate that, not only on the mesh spaces but also on the grid area, the hybrid film effectively contours the whole TEM grid surface with ordered BF arrays (Fig. 2a and 2b). This result reveals that the T_g of the polymer may not be the exclusive factor which influences the formation of 3D microporous films on nonplanar substrates. A detailed description of the formation of microporous polymer (hybrid) films on nonplanar substrates with such rod–rod copolymers will be published elsewhere. Once peeled off the grid by a tweezer, multi-level surface features are formed on the substrate, originating from the self-assembly of water droplets, and the pattern of the TEM grid (Fig. 2c). As reported in our previous publications, a single layer of the microporous film is necessary for the formation of ordered inorganic micropatterns.[7d] The cross-sectional view (Fig. 2d)

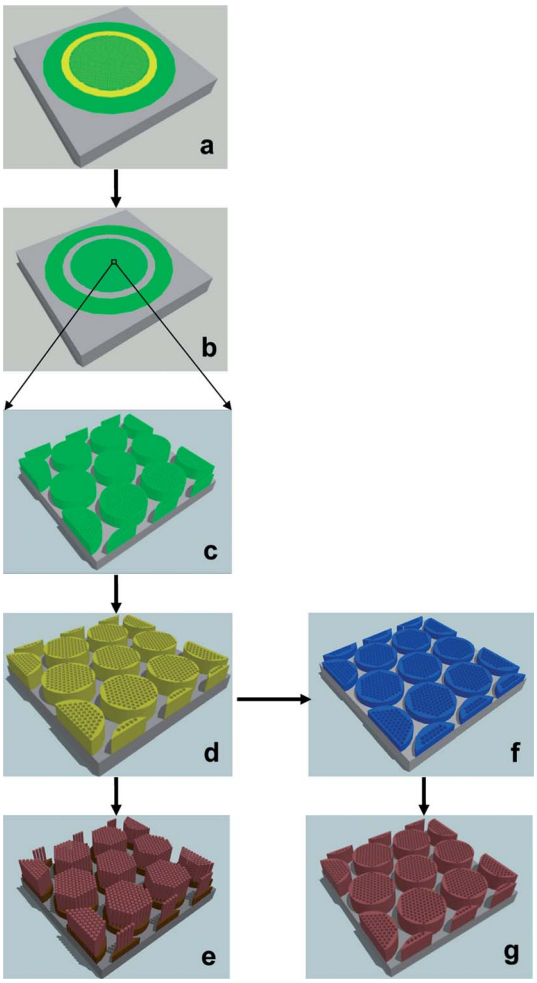

Fig. 1 Schematic pictures of fabrication process of multi-level CNT arrays with adjustable patterns on a substrate. (a) A droplet of PSPAA/ferrocene solution was cast onto the Si substrate covered with a TEM grid using a microsyringe; (b) the TEM grid was removed after total evaporation of the solvent under high humidity; (c) a two-level microporous hybrid film was formed on the substrate; (d) the polymer matrix was cross-linked by ultraviolet irradiation and the two-level honeycomb structures were well preserved after the photochemical process; (e) two-level isolated CNT bundles were developed templating from the cross-linked microporous polymer film; (f) two-level ferrous inorganic micropatterns in honeycomb structures were formed on the substrate after pyrolysis; (g) two-level dense CNT arrays with a hexagonal shape were formed, guided by the inorganic micropatterns.

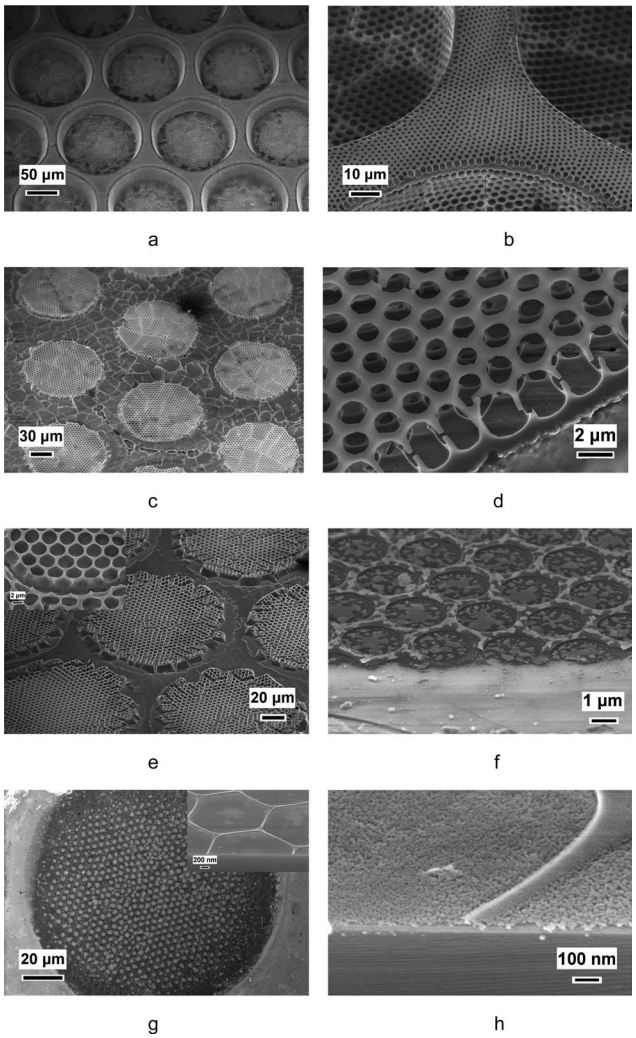

Fig. 2 (a) SEM image of an ordered porous PSPAA/ferrocene hybrid film formed on the surface of a 150 mesh hexagonal TEM grid; (b) magnified image of (a); (c) a two-level microporous PSPAA/ferrocene hybrid film on the substrate after removing the TEM gird; (d) a cross-section view of the honeycomb structured PSPAA/ferrocene hybrid film; (e) SEM image of the two-level honeycomb structured PSPAA/ferrocene hybrid film after 4 h ultraviolet irradiation, the inset shows a cross-sectional view; (f) a cross-section view of the cross-linked PSPAA/ferrocene hybrid film after heating at 750 °C for 10 min; (g) SEM image of the two-level ferrous inorganic micropattens after pyrolyzing the cross-linked hybrid film at 450 °C for 5 h, the inset shows a magnified image; (h) close examination of the formed inorganic micropattens, indicating that the hexagonal edges are isolated from the Si substrate.

reveals that the resultant film has a monolayer of independent pores on the dense polymer stratum without network structures. The successful preparation of multi-level microporous hybrid films indicates that non-planar substrate does not alter the behavior of PSPAA/ferrocene during the static BF process.

Block copolymers (BCPs) are believed to be super structure-directing agents in solution, in the bulk and on surfaces, thanks to their amphiphilic character. The synthesis of organic/inorganic hybrid materials using BCPs as structure-directing agents or templates is an area of rapid growth.[10] For example, highly-ordered nanostructured silica (MCM41 and SBA15) has been developed by templating from commercially available triblock copolymers, Pluronics.[11] However, in order to use the as-prepared microporous hybrid film as a template to guide the following CVD growth, some further treatments are needed to increase its thermal stability, because CVD growth demands relatively high temperature at which the film will melt and its microstructures will totally disappear. Cross-linking should be an efficient method for stabilizing the film structure against solvents and heat annealing.[12] Either PS or PAA composition can be effectively cross-linked under deep ultraviolet irradiation, as discussed in our previous research.[7a] Therefore, the microporous hybrid film was firstly treated with ultraviolet irradiation, and the SEM image shown in Fig. 2e demonstrates that the structures in the hybrid film were maintained after the photochemical process. After cross-linking, since the unzipping and depropagation reactions of the block polymer were strongly prohibited, the thermal decomposition rate of the macromolecular chains was slowed down. As revealed by the thermogravimetric (TG) results (see the ESI†), the char yield of cross-linked PSPAA was close to 40%, even when heated up to 450 °C at a rate of 5 °C min^{-1} in an air atmosphere. The microstructures on the cross-linked hybrid film were found to survive after thermal treatment at 750 °C for 10 min (the same condition in CVD, Fig. 2f), indicating that the cross-linked film was applicable to the further CVD growth. From the SEM images, some changes in the morphology of the film can also be observed after annealing. The film thickness was found to shrink significantly, because the photochemical cross-linking occurs mostly on the film surface, and the less cross-linked polymer stratum collapses during annealing. SEM observation (Fig. 2g) reveals that the walls of the obtained inorganic micropattern become thinner and sharper, suggesting that much material was burned out. In fact, the core scan of Fe (see the ESI†) definitely shows that the incorporated ferrocene has been oxidized to Fe_2O_3. Therefore, pyrolysis decomposes the polymer matrix and converts the incorporated ferrocene into Fe_2O_3, leaving the skeleton of inorganic micropatterns. The formed micropatterns have the identical spacing with that of the micropores on the as-prepared film surface, indicative of the *in situ* formation of inorganic patterns on the honeycomb structures. The cross-linked polymer matrix and the ferrous inorganic micropatterns are used to template the multi-level CNT growth with adjustable arrays as discussed below.

To grow CNT on the micropatterned templates, CVD was carried out. The deposition was operated under a constant flow rate of $Ar/H_2/C_2H_2$ with 500/200/78 standard-state cubic centimetre per minute (sccm), while the growth temperature was 750 °C and the time was 10 min. To avoid the undesired reactions during the ramping step, the Si wafers with template were kept at the cool end of the furnace until the temperature of the furnace reached the predetermined working value. When C_2H_2 gas was induced into the reactor carried by Ar and H_2, CNTs began to grow from the micropatterned templates. Two different CNT arrays can be prepared, depending on the template used. If the cross-linked hybrid film was used as template (Fig. 2e), isolated CNT bundles would form from the cavities of the film (Fig. 3a), and were isolated by the walls of the honeycomb structures (Fig. 3b and 3c). The high-resolution (HR) TEM image definitely shows that the formed CNTs are multi-walled tubes with an

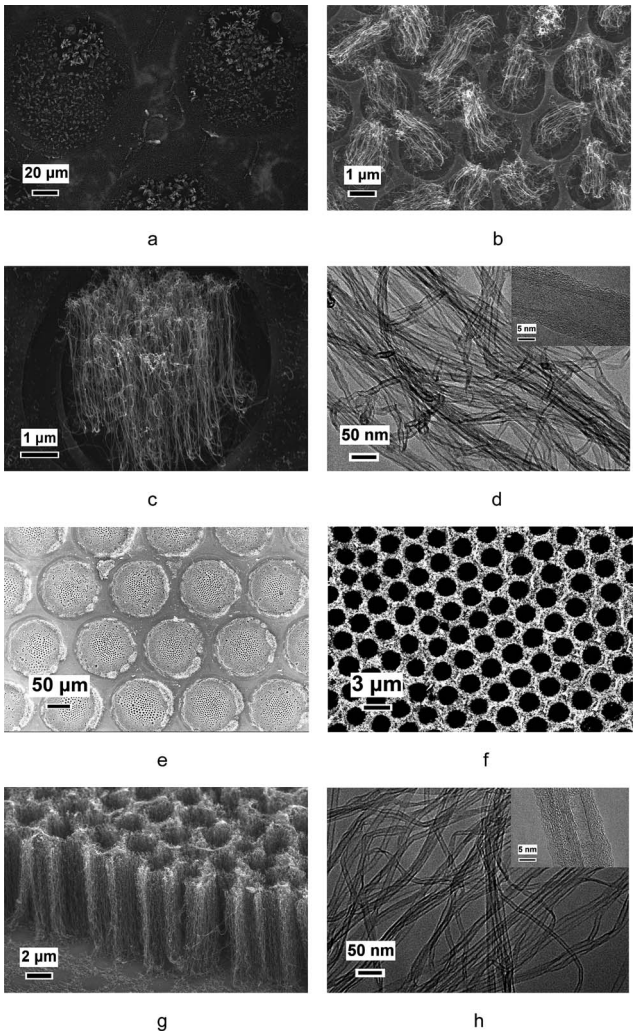

Fig. 3 SEM images of the hierarchically isolated CNT bundles in hexagonal arrays developed from the cavities: (a) top view, (b) magnified image of (a) and (c) side view; (d) a TEM image of the patterned CNTs in Fig. 3a, the inset shows HRTEM view of one multi-walled CNT. SEM images of the hierarchically dense CNT bundles with a honeycomb structure perpendicular to the substrate, (e) top view, (f) magnified image of (e) and (g) side view; (h) a TEM image of the patterned CNTs. In Fig. 3e, the inset shows a HRTEM view of one multi-walled CNT.

average diameter of 15 nm (Fig. 3d and the inset). Either the CVD temperature or carbon feedstock can have an influence on the formation of single- or multiple-wall CNTs. As pointed by Coville and Campbell,[13] low CVD temperature (below 750 °C) and acetylene feedstocks facilitate the growth of multi-wall carbon nantotubes. Since the CVD temperature is 750 °C and carbon source is acetylene in our experiment, we just obtain multi-wall carbon nantotube arrays. If ordered ferrous inorganic micropattens were used as the template in the CVD growth (Fig. 2g), a honeycomb-like skeleton of dense CNT bundles would form, as shown in Fig. 3e and 3f. The spacing of the skeleton is identical with that of the inorganic micropatterns, indicating an *in situ* inorganic pattern formation on the honeycomb structures. The cross-sectional view demonstrates that the aligned CNTs are perpendicular to the substrate without collapse (Fig. 3g), because the supporting force among the continuous CNT bundles counteracted the effect of gravity.[14] The well-aligned CNT bundles have a uniform length of 8 μm and this length can be controlled by changing the time of CVD. The HRTEM image of the formed CNTs is shown in Fig. 3h.

The pattern of CNT is determined by that of the Fe catalyst on the substrate, therefore, the formation of multi-level CNT arrays with adjustable patterns results from the different distribution of catalyst in the cross-linked hybrid film and ferrous inorganic micropatterns (a schematic illustration is shown in the ESI†). Ferrocene has strong intermolecular interaction with aromatic molecules and polar groups because of its molecular structure.[15] The added ferrocene should disperse into the polymer matrix uniformly. However, the selective growth of isolated CNT bundles from the cavities is attributed to the selective interfacial aggregation of ferrocene on the walls of the cavities, resulting from the Pickering emulsion effect,[16] a common phenomenon in which emulsion can be stabilized by solid particles adsorbing onto the interface. In a typical BF formation process, water droplets floating on the surface of the solution are arranged into highly ordered arrays. Hence it introduces patterned liquid/liquid phase interfaces which can be utilized to control the assembly and alignment of ferrocene particles. Before the polymer film becomes too viscous, the ferrocene particles aggregate at the interface and form a uniform layer. As the concentration of the polymer/ferrocene mixture increases with solvent evaporation, the polymer film undergoes glass transition and solidifies, fixing the droplets and the ferrocene particles. On evaporation of the water, spherical cavities remain with the walls decorated by the ferrocene particles.[17] After crosslinking of the polymer film by ultraviolet irradiation, the ferrocene particles are either located on the walls of the cavities or embedded in the hybrid film. Upon H_2 treatment, ferrocene particles exposed on the cavity walls are reduced and become activated to catalyze the growth of CNTs in the cavities. However, the ferrocene particles embedded in the hybrid film are isolated from H_2 and acetylene gas (carbon source). As a result, we have been able to achieve the selective growth of CNTs in the cavities. The change of CNT arrays from isolated bundles to continuous CNT honeycomb structures is explained as follows. During pyrolysis, the polymer matrix is gradually decomposed and the cavity bottoms sink down onto the substrate, while a chemical reaction occurs between the Si wafer and ferrocene at high temperature.[18] This results in a complete change in the chemical nature of the active ferrocene catalyst to stable compounds such as iron silicide ($FeSi_2$) and iron silicate (Fe_2SiO_4), which are known for their noncatalytic activity for CNT growth.[19] Although a 2-nm thick native oxide layer was examined to exist on the commercially available Si wafer (determined by ellipsometry in our lab), it cannot prevent Fe from diffusing through it and reacting with the Si substrate.[20] On the other hand, the ferrocene particles embedded in the polymer matrix, especially on the hexagonal edges, are oxidized and exposed to the surface because most of the polymer composition has been burned off during pyrolysis. The close SEM view, as shown in Fig. 2h, indicates that the height difference between the edges and bottoms of the inorganic micropatterns is 50 nm, which is thick enough to isolate the ferrous micropatterns from the Si substrate. Although ferrocene is oxidized into Fe_2O_3, they still can be reduced [21] and effectively catalyze the growth of highly dense CNTs.

The beauty of this process is that a number of different patterns can be obtained simply by choosing different TEM grids,

therefore it is easily scaled up to large area. To highlight these patterning technologies, we utilized TEM grids with different sizes and shapes to construct multi-level surface features (100 mesh, square pattern and 200 mesh, square pattern). The resultant multi-level CNT arrays with two level orders are displayed in Fig. 4.

Conclusions

We have prepared multi-level microporous PSPAA/ferrocene hybrid films guided by TEM grids through the static BF process. Films with two levels of ordered features were obtained. One level originates from the contour of the templates, while the other originates from the condensation of water droplets (BF arrays). After cross-linking by ultraviolet irradiation, the microporous film can be converted into the ordered inorganic micropatterns by pyrolysis, during which the incorporated ferrocene was converted into Fe_2O_3 and replaced the skeleton of polymer. Two types of multi-level CNT patterns, isolated CNT bundles (starting from cross-linked hybrid film) and honeycomb-structured dense CNT arrays (templating from ferrous inorganic micropatterns), were created after CVD. The formation of the isolated CNT bundles is attributed to the selectively interfacial aggregation of the catalyst ferrocene to the walls of the cavities, whereas the dense CNT arrays in hexagonal shape is believed to develop from the catalytic ferrous inorganic micropatterns. The beauty of this process is that a number of different patterns can be obtained simply through the choice of TEM grids. This flexible and low-cost strategy offers a controllable way to fabricate large-area multi-level CNT patterns with unique geometry.

Experimental

Materials

Amphiphilic diblock copolymer PSPAA was synthesized by atom transfer radical polymerization in a similar procedure as reported in ref. 22. The relative molecular weights of PS and PAA blocks were 9000 and 2500 g mol^{-1}, respectively. The molecular weight distribution (M_w/M_n) of such diblock copolymer was 1.07. Ferrocene and CS_2 were purchased from Shanghai Chemical Reagent Plant. All the chemical reagents were used without further purification. Si wafers and TEM grids were used as-received.

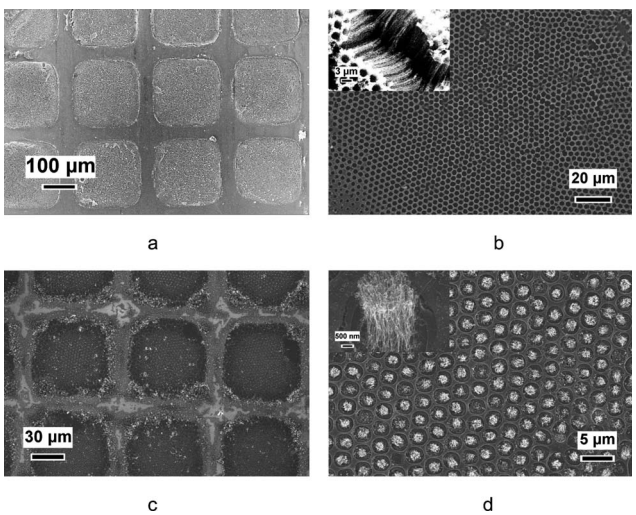

Fig. 4 SEM images of two-level CNT arrays templating from the TEM grids with different mesh sizes and patterns: (a) 100 mesh TEM grid with square pattern; (b) magnification of (a), the inset shows the side view with higher magnification; (c) 200 mesh square TEM grid; (d) magnification of (c). The inset in (d) shows a single bundle of CNTs.

Preparation of honeycomb structured hybrid films

The static BF process was operated in a 25 mL straight-mouth glass bottle with a cap. A saturated relative humidity in the vessel was achieved by adding 2 mL of distilled water into the bottle beforehand. A piece of Si substrate was adhered onto the top of a plastic stand with a double-sided tape and placed into the glass vessel. The substrate was 1 cm higher than the liquid level. A piece of TEM grid was placed onto the center of the Si substrate. PSPAA and ferrocene were mixed with a fixed weight ratio (5 : 1, w/w) and dissolved in CS_2. The solution concentration was 15 mg mL^{-1}. The honeycomb film was prepared by casting 100 μL of solution onto the grid with a microsyringe. After complete evaporation of CS_2, the TEM grid was peeled off carefully from the substrate. The surface feature of the substrate was observed by SEM. All the experiments were carried out at room temperature unless stated otherwise.

Preparation of multi-level micro-structured ferric oxide templates

The hybrid microporous film was photo-chemically cross-linked by exposing the film to ultraviolet light at 30 °C in air, using a UVO cleaner (ZWLH-5, Tianjin, China). The cleaner generated ultraviolet emission with wavelength of 254 nm and power of 500 W. The distance between the ultraviolet source and the film surface was 10 cm. After 4 h ultraviolet exposure, the cross-linked film was heated to 450 °C in 2 h and held for another 5 h under an air atmosphere. During the pyrolysis, ferrocene turned into oxide and replaced the polymer skeleton eventually.

Preparation of CNT arrays

Aligned CNT arrays were synthesized by thermal CVD in a 40 mm diameter quartz tube furnace. The tube furnace was pre-heated to 750 °C and then the templates were inserted into the chamber. An Ar/H_2 gas mixture was used as the buffer gas and pure acetylene served as the carbon source. In the growth process, a constant flow rate of 500/200/78 sccm for $Ar/H_2/C_2H_2$ was used. The growing time was 10 min.

Characterization and apparatus

The relative molecular weights and M_w/M_n of PSPAA were measured by a Waters gel permeation chromatography (GPC) system equipped with a Waters 1515 Isocratic HPLC pump, a Waters 2414 refractive index detector, a Waters 2487 dual λ absorbance detector (UV) and a set of Waters Styragel columns. GPC measurements were carried out at 35 °C using tetrahydrofuran as an eluent with a flow rate of 1.0 mL min^{-1}. The system was calibrated with polystyrene standards. The morphology and structure of patterned CNTs were characterized by a Hitachi

S4800 SEM. A 10 keV electron beam was used for the observation with a working distance of 8 mm in order to obtain secondary electron images. X-Ray photoelectron spectroscopy spectra were acquired with a PHI Quantum 2000 spectrometer using monochromated X-rays from an Al Kα source with a takeoff angle of 45° from the surface plane. The morphology and structure of the CNTs were characterized by HRTEM (TECNAI F-30) with an acceleration voltage of 300 kV. The TEM specimens were prepared by dispersing the CNTs in ethanol and deposited a drop of the dispersion on a carbon-film-coated copper grid. TG analysis was taken on a Netzsch STA 409 EP Thermal Analyzer in a nitrogen atmosphere.

Acknowledgements

L. Li gratefully acknowledges the National Natural Science Foundation of China (No. 50703032, 51035002 and 20974089) and the Program for New Century Excellent Talents of Ministry of Education of China (NCET-08-0475) and Natural Science Foundation of Fujian Province (2009J06029).

References

1 M. S. Dresselhaus, G. Dresselhaus, J. C. Charlier and E. Hernández, *Philos. Trans. R. Soc. London, Ser. A*, 2004, **362**, 2065.
2 (*a*) S. S. Fan, M. G. Chapline, N. R. Franklin, T. W. Tombler, A. M. Cassell and H. J. Dai, *Science*, 1999, **283**, 512; (*b*) B. Q. Wei, R. Vajtai, Y. Jung, J. Ward, R. Zhang, G. Ramanath and P. M. Ajayan, *Nature*, 2002, **416**, 495; (*c*) K. Hata, D. N. Futaba, K. Mizuno, T. Namai, M. Yumura and S. Iijima, *Science*, 2004, **306**, 1362.
3 (*a*) J. H. Hafner, C. L. Cheung and C. M. Lieber, *Nature*, 1999, **398**, 761; (*b*) D. N. Futaba, K. Hata, T. Yamada, T. Hiraoka, Y. Hayamizu, Y. Kakudate, O. Tanaike, H. Hatori, M. Yumura and S. Iijima, *Nat. Mater.*, 2006, **5**, 987; (*c*) J. M. Bonard, T. Stöckli, O. Noury and A. Châtelain, *Appl. Phys. Lett.*, 2001, **78**, 2775; (*d*) J. Q. Huang, Q. Zhang, M. Q. Zhao, G. H. Xu and F. Wei, *Nanoscale*, 2010, **2**, 1401; (*e*) L. T. Qu, R. A. Vaia and L. M. Dai, *ACS Nano*, 2011, **5**, 994; (*f*) J. Koehne, H. Chen, J. Li, A. M. Cassell, Q. Ye, H. T. Ng, J. Han and M. Meyyappan, *Nanotechnology*, 2003, **14**, 1239; (*g*) S. S. Fan, M. G. Chapline, N. R. Franklin, T. W. Tombler, A. M. Cassell and H. J. Dai, *Science*, 1999, **283**, 512; (*h*) S. J. Kang, C. Kocabas, S. HoKim, Q. Cao, M. A. Meitl, D. Y. Khang and J. A. Rogers, *Nano Lett.*, 2007, **7**, 3343.
4 (*a*) R. D. Bennett, A. J. Hart, A. C. Miller, P. T. Hammond, D. J. Irvine and R. E. Cohen, *Langmuir*, 2006, **22**, 8273; (*b*) K. B. K. Teo, M. Chhowalla, G. A. J. Amaratunga, W. I. Milne, P. Legagneux, G. Pirio, L. Gangloff, D. Pribat, V. Semet, V. T. Binh, W. H. Bruenger, J. Eichholz, H. Hanssen, D. Friedrich, S. B. Lee, D. G. Hasko and H. Ahmed, *J. Vac. Sci. Technol., B*, 2003, **21**, 693; (*c*) S. Lastella, Y. J. Jung, H. C. Yang, R. Vajtai, P. M. Ajayan, C. Y. Ryu, D. A. Rider and I. Manners, *J. Mater. Chem.*, 2004, **14**, 1791; (*d*) S. M. C. Vieira, K. B. K. Teo, W. I. Milne, O. Groning, L. Gangloff, E. Minoux and P. Legagneux, *Appl. Phys. Lett.*, 2006, **89**, 022111.
5 G. Widawski, M. Rawieso and B. François, *Nature*, 1994, **369**, 387.
6 (*a*) U. H. F. Bunz, *Adv. Mater.*, 2006, **18**, 973; (*b*) M. H. Stenzel, C. Barner-Kowollik and T. P. Davis, *J. Polym. Sci., Part A: Polym. Chem.*, 2006, **44**, 2363.
7 (*a*) L. Li, C. K. Chen, A. J. Zhang, X. Y. Liu, K. Cui, J. Huang, Z. Ma and Z. H. Han, *J. Colloid Interface Sci.*, 2009, **331**, 446; (*b*) L. Li, Y. W. Zhong, C. Y. Ma, J. Li, C. K. Chen, A. J. Zhang, D. L. Tang, S. Y. Xie and Z. Ma, *Chem. Mater.*, 2009, **21**, 4977; (*c*) C. Y. Ma, Y. W. Zhong, J. Li, C. K. Chen, J. L. Gong, L. Li, Z. Ma and S. Y. Xie, *Chem. Mater.*, 2010, **22**, 2367; (*d*) L. Li, J. Li, Y. W. Zhong, C. K. Chen, Y. Ben, J. L. Gong and Z. Ma, *J. Mater. Chem.*, 2010, **20**, 5446; (*e*) L. Li, C. K. Chen, J. Li, A. J. Zhang, X. Y. Liu, B. Xu, S. B. Gao, G. H. Jin and Z. Ma, *J. Mater. Chem.*, 2009, **19**, 2789; (*f*) L. Li, Y. W. Zhong, J. L. Gong, J. A. Li, C. K. Chen, B. R. Zeng and Z. Ma, *Soft Matter*, 2011, **7**, 546; (*g*) L. Li, Y. W. Zhong, J. Li, C. K. Chen, A. J. Zhang, J. Xu and Z. Ma, *J. Mater. Chem.*, 2009, **19**, 7222.
8 (*a*) L. A. Connal, R. Vestberg, C. J. Hawker and G. G. Qiao, *Adv. Funct. Mater.*, 2008, **18**, 3315; (*b*) L. A. Connal, R. Vestberg, P. A. Gurr, C. J. Hawker and G. G. Qiao, *Langmuir*, 2008, **24**, 556; (*c*) L. A. Connal and G. G. Qiao, *Adv. Mater.*, 2006, **18**, 3024; (*d*) L. A. Connal and G. G. Qiao, *Soft Matter*, 2007, **3**, 837.
9 J. E. Mark, *Polymer Data Handbook*, Oxford University, New York, 1999.
10 (*a*) O. Karthaus, X. Cieren, N. Maruyama and M. Shimomura, *Mater. Sci. Eng., C*, 1999, **10**, 103; (*b*) K. Zhang, L. W. Zhang and Y. M. Chen, *Macromol. Rapid Commun.*, 2007, **28**, 2024; (*c*) B. C. Englert, S. Scholz, P. J. Leech, M. Srinivasarao and U. H. F. Bunz, *Chem.–Eur. J.*, 2005, **11**, 995.
11 (*a*) D. Y. Zhao, J. L. Feng, Q. S. Huo, N. Melosh, G. H. Fredrickson, G. D. Stucky and B. F. Chmelka, *Science*, 1998, **279**, 548; (*b*) J. Fan, C. Z. Yu, F. Gao, J. Lei, B. Z. Tian, L. M. Wang, Q. Luo, B. Tu, W. Z. Zhou and D. Y. Zhao, *Angew. Chem.*, 2003, **115**, 3254; (*c*) C. Z. Yu, J. Fan, B. Z. Tian, D. Y. Zhao and G. D. Stucky, *Adv. Mater.*, 2002, **14**, 1742; (*d*) J. Lee, J. Kim and T. Hyeon, *Adv. Mater.*, 2006, **18**, 2073; (*e*) Y. M. Wang, Z. Y. Wu, L. Y. Shi and J. H. Zhu, *Adv. Mater.*, 2005, **17**, 323.
12 (*a*) H. Yabu, M. Kojima, M. Tsubouchi, S. Onoue, M. Sugitani and M. Shimomura, *Colloids Surf., A*, 2006, **284–285**, 254; (*b*) B. Erdogan, L. L. Song, J. N. Wilson, J. O. Park, M. Srinivasarao and U. H. F. Bunz, *J. Am. Chem. Soc.*, 2004, **126**, 3678; (*c*) O. Karthaus, Y. Hashimoto, K. Kon and Y. Tsuriga, *Macromol. Rapid Commun.*, 2007, **28**, 962.
13 (*a*) V. O. Nyamori, S. D. Mhlanga and N. J. Coville, *J. Organomet. Chem.*, 2008, **693**, 2205; (*b*) F. Rohmund, L. K. L. Falk and E. E. B. Campbell, *Chem. Phys. Lett.*, 2000, **328**, 369.
14 J. Wu, Q. W. Huang, Y. F. Ma, Y. Huang, Z. F. Liu, X. Y. Yang, D. P. Chen and Y. S. Chen, *Colloids Surf., A*, 2008, **313–314**, 13.
15 (*a*) X. Y. Yang, Y. H. Lu, Y. F. Ma, Y. J. Li, F. Du and Y. S. Chen, *Chem. Phys. Lett.*, 2006, **420**, 416; (*b*) S. Y. Guo and Y. Ning, *J. Polym. Sci., Part B: Polym. Phys.*, 1999, **37**, 2828.
16 S. U. Pickering, *J. Chem. Soc. Trans.*, 1907, **91**, 2001.
17 (*a*) A. Böker, Y. Lin, K. Chiapperini, R. Horowitz, M. Thompson, V. Carreon, T. Xu, C. Abetz, H. Skaff, A. D. Dinsmore, T. Emrick and T. P. Russell, *Nat. Mater.*, 2004, **3**, 302; (*b*) W. Sun, J. C. Shen and J. Ji, *Langmuir*, 2008, **24**, 11338.
18 Y. J. Jung, B. Q. Wei, R. Vajtai and P. M. Ajayan, *Nano Lett.*, 2003, **3**, 561.
19 T. de los Arcos, F. Vonau, M. G. Garnier, V. Thommen, H. G. Boyen, P. Oelhafen, M. Düggelin, D. Mathis and R. Guggenheim, *Appl. Phys. Lett.*, 2002, **80**, 2383.
20 A. Y. Cao, P. M. Ajayan, G. Ramanath, R. Baskaran and K. Turner, *Appl. Phys. Lett.*, 2004, **84**, 109.
21 A. Pineau, N. Kanari and I. Gaballah, *Thermochim. Acta*, 2006, **447**, 89.
22 Y. J. Kang and T. A. Taton, *Angew. Chem., Int. Ed.*, 2005, **44**, 409.